ISSN: 2583-9292 (ONLINE)
DOI: 10.21917/ijdsml.2026.0186

INTEGRATING INTERNET OF THINGS-CONNECTED WEARABLE DEVICES FOR PATIENT MONITORING USING DEEP SPARSE AUTOENCODER AND OPTIMISATION ALGORITHM IN SMART HEALTHCARE

A.N. Swamynathan[1] and S. Thirumal[2]
[1]Department of Computer Science, Rajeswari Vedachalam Government Arts College, India
Department of Computer Science, Arignar Anna Government Arts College, Cheyyar, India

Abstract

Health is a significant factor in life. Still, people failed to get the right health care services. It is caused by restrictions on the technology used in hospitals and on access to hospitals. The Internet of Things (IoT) is a hot topic nowadays, offering many solutions across various sectors, for example, in healthcare. IoT is applied in several health interventions, including identifying illness as a protection, treating illness as a healing process, and monitoring illness as a healing solution itself. The wearable sensors utilised for monitoring blood pressure and heart rate are proven to distinguish in the initial stage. At present, deep learning (DL) techniques in this domain are promising methods for improving patient care. In this manuscript, we propose an effective Patient Monitoring with Wearable Devices Using Deep Sparse Autoencoder and Optimisation Algorithm (PMWD-DSAEOA) model in smart healthcare. The aim is to develop an effective framework for real-time health monitoring utilising wearable devices to enable proactive, personalised healthcare solutions. To accomplish that, the PMWD-DSAEOA model includes a data pre-processing step that normalises the input data using Z-scores for effective analysis. Next, the feature selection step is used, a critical stage that reduces data dimensionality and improves efficiency by implementing the northern goshawk optimisation (NGO) method. Additionally, the classification process primarily uses the stacked sparse autoencoder (SSAE) method. To further improve the model's performance, the dung beetle optimisation (DBO) method is employed for parameter tuning. To demonstrate the improved performance of the PMWD-DSAEOA approach, a comprehensive experimental study is conducted. The comparative outcomes indicated the improved features of the PMWD-DSAEOA approach.

Keywords:

Patient Monitoring, Internet of Things, Wearable Devices, Smart Healthcare, Dung Beetle Algorithm, Deep Learning, Deep Sparse Autoencoder

1. INTRODUCTION

Healthcare these days requires significant investment in technology, which is becoming more expensive and more complicated to obtain. Similar to rural towns, hospitals in rural areas lack the technologies found in urban hospitals. City hospitals lack the time to meet patients' needs; therefore, they must transfer to other hospitals in different cities or travel to other countries to access the health technologies they require [1]. The IoT in healthcare is widely needed to make it easier for humans to manage, detect, monitor, and take action upon receiving data in the system, and to reduce healthcare expenses efficiently.

IoT devices are computers with microcontrollers, transceivers, and sensors. These elements interconnect among themselves to present a variety of data that can assist the client [2]. Therefore, IoT is among the most popular subjects in computer technology. In IoT, healthcare offers a potential to enhance the technologies utilised today and reduce the cost of each healthcare feature. IoT customer-oriented services, such as smartphones and portable devices, have become very popular among people for health monitoring in smart healthcare. IoT-helped portable sensor systems technology is a growing area in medical systems. According to the healthcare sector, doorstep analysis, effortless supervision, and effective information management are required [3]. Portable devices process and analyse information gathered from humans to enhance their standard of living [4]. In general, Portable IoT can work with several motion sensors that capture images throughout the day of an individual's physical activities and life signs, and sync with their mobile device or other smart devices [5].

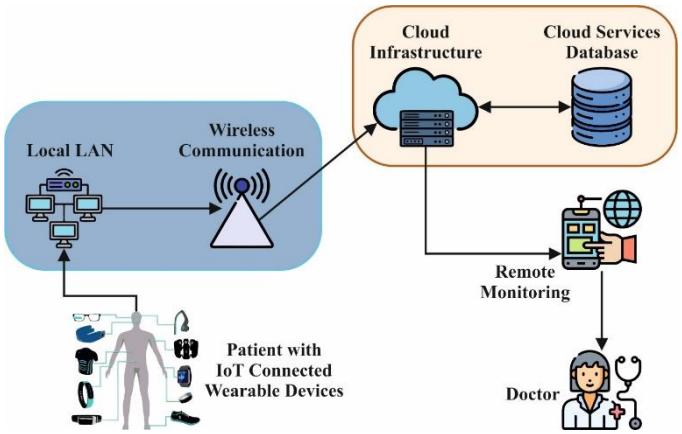

Fig.1. General process of IoT-healthcare

These smart devices take many forms, including skin patches, smart rings, smart jewellery, smart glasses, smart clothes, and other products, focusing on specific aspects of customer health by efficiently gathering and processing information [6]. Moreover, continuous digital monitoring of human health over a lifetime is among the most significant advantages of IoT devices and portable devices, and the growing prevalence of utilising portables and the development of the intersection of the digital and physical worlds in the IoT field [7]. Though most portable and IoT devices are intended to measure specific details of a person's primary health range, such as temperature, physical activity, blood pressure, heart rate, calories burnt, or respiratory symptoms, and monitor coughing [8].

Currently, artificial intelligence (AI) methods in the subject have shown potential approaches for enhancing patients' healthcare. Frequently, machine learning (ML) methods are favoured owing to their ability to deliver more precise and rapid results at lower computational cost [9]. ML also enables portable devices to make automatic decisions without explicit

programming tailored to a specific scenario, by utilising information from past experiences [10].

Several healthcare and advanced care applications utilise ML techniques like arrhythmia detection, seizure detection, activity recognition, fall detection, disease diagnoses, stress detection, emotion recognition, and rehabilitation challenges, DL techniques relate to ML, and they consent to improve the predictive characteristic because of their inherent capability to both combine information from several sources and deal with vast volumes of data [11]. The Fig.1 illustrates the general process of IoT healthcare.

This manuscript proposes an effective patient monitoring system using wearable devices, based on a deep sparse autoencoder and Optimisation Algorithm (PMWD-DSAEOA) in Smart Healthcare. The contributions of this paper are concluded as follows:

- This paper develops an effective framework for real-time health monitoring utilising wearable devices to enable proactive, personalised healthcare solutions.
- Primarily, the Z-score normalisation is applied during data preparation to standardise the input data for effective analysis.
- Consequently, the feature selection step is applied to reduce data dimensionality and improve efficiency using the NGO method.
- Furthermore, the classification process is mainly executed by the SSAE model.
- To further enhance the model performance, the DBO approach is used for parameter tuning.
- The comparative results represented the improved features of the PMWD-DSAEOA method.

2. RELATED WORKS ON IOT-BASED HEALTHCARE DATA

Anjum et al. [12] presented an Opportunistic Access Control Scheme (OACS) for employing security at the access level. It is a scheme where user permissions depend on their needs and the data. Upon accessing health records, a central IoT security augmentation and evaluation is provided. The presented scheme examines potential delegation techniques to enable users to access their healthcare records without interruption. Rafique [13] introduced an ML-RASPF, an ML-driven approach for effectual service delivery in the smart healthcare system. In contrast to current techniques, ML-RASPF cooperatively improves latency and service delivery rates through adaptive control and predictive analytics in modular mist-edge-cloud systems. This system frames task provisioning as a joint optimisation problem that minimises service latency and optimises delivery capacity. Aldosary and Tanveer [14] proposed a physical unclonable function (PUF) and authentication network for IoT-based SHS, termed PAAF-SHS. It enables encrypted, secure communication among medical servers and users after mutual authentication. The PUF is integrated into medical servers and IoT-based devices to enhance resilience against internal attackers and potential key attacks on medical servers. Rahman et al. [15] presented a structural design integrating SDN and Blockchain (BC) technologies. This architecture is specifically designed to enable remote patient monitoring systems in 5G settings. This architectural framework comprises a patient-centric agent (PCA) within the Software-Defined Network (SDN) control plane to manage user data on the patient's behalf. The PCA enables the proper management of patient data by delivering essential instructions to the forwarding devices. In [16], multi-model IoT (MMIoT) devices are leveraged to concurrently monitor and collect health data from various body parts. Moreover, the long short-term memory (LSTM) and U-Net models are utilised to automatically examine the data. Data pre-processing is performed by the server linked to the MMIoT networks. The results from LSTMs and U-Nets are fed into a dense layer for precise classification of health abnormalities.

Irshad et al. [17] presented an innovative whale-driven attribute encryption scheme (WbAES) that enables the transmitter and receiver to encrypt and decrypt data. The presented model uses attribute-based encryption (ABE) employing the whale optimiser algorithm (WOA) to determine the appropriateness of the whale's behaviour, thereby generating appropriate secret and master public keys, guaranteeing security against illegal access and use. Gharaei et al. [18] designed an edge-based companion-side eHealth monitoring method for smart hospitals. In many current edge-based eHealth monitoring models, the employed edge devices have insufficient storage capacity and energy resources, leading to network failures and data packet loss. Thus, initially, edge-based health assessors were utilised to receive medical signals from biosensors at regular intervals and to evaluate patient health conditions. Paulraj et al. [19] proposed a pivotal study on a "Smart Healthcare Monitoring System" that leverages these technologies for real-time patient examination. With the growing need for precise, immediate medical evaluations, this study addresses the critical need for early and accurate diagnosis. This suggested system integrates IoT-driven wearable sensors and devices to extract comprehensive patient data. A hybrid model is deployed to leverage this data, combining a DL approach with the XGBoost method to enable faster decision-making. The literature review of IoT-enabled healthcare monitoring using a wearable device is given in Table 1.

Table.1. Review of IoT-enabled healthcare monitoring

Authors	Objectives	Techniques	Outcomes
Anjum et al. [12]	To present a method for defendable access control of user permissions based on their necessity and information.	OACS	Reduces false rates by 11.74%.
Rafique [13]	To propose an innovative approach for latency-aware and rate-adaptive IoT service supplying in smart medical care approaches.	ML-RASPF	Delivery rate of 18%.
Aldosary and Tanveer [14]	To present data security for IoT-assisted gadgets with confined resources.	PAAF-SHS	Computation Cost from 4.78% to 68.98%.
Rahman et al. [15]	To examine the structural framework	BC, PCA, SDN	Achieves throughput

	that incorporates BC technology.		and packet error rate.
Balasundaram et al. [16]	To identify and gather clinical information from various body parts concurrently.	LSTM, U-Net	NA
Irshad et al. [17]	To increase safety and evade attacks, employing an energy-efficient model to diminish energy consumption in computation.	WbAES, ABE, WOA	Accuracy of 99.85 %.
Gharaei et al. [18]	Advancing eHealth monitoring methods for smart hospitals depends on IoT.	eHealth Monitoring Method	Achieves 99%.
Paulraj et al. [19]	To introduce a method that integrates IoT-enabled wearable sensors and devices to acquire comprehensive patient information.	DL, XGBoost	Accuracy of 87.5%.

3. METHODOLOGY FRAMEWORK

In this paper, a PMWD-DSAEOA model is proposed in smart healthcare. The paper aims to design an effective system for real-time health monitoring using wearable devices to enable proactive, tailored healthcare solutions. To perform this, the PMWD-DSAEOA model comprises the following processes: an input data processing phase, feature reduction via the NGO model, classification, and DBO-based parameter tuning. The Fig.2 depicts the overall workflow of the PMWD-DSAEOA method.

3.1 Z-SCORE STANDARDIZATION

Initially, the data preparation step uses Z-score standardisation to normalise the input data for effective analysis. The data normalisation model converts the data to the range [0, 1] using the mean and standard deviation [20]. To be clearer, it is formally applied to data attributes with different scales. For example, the data point is represented as s_j; the equation of z-score normalisation is measured as

$$ZN_j = \frac{s_j - \sigma}{p} \tag{1}$$

where, the data point is represented by s_j, and ρ and σ represent the dataset's mean and standard deviation.

3.2 FEATURE REDUCTION USING NGO MODEL

Then, the feature selection step is applied to reduce data dimensionality and improve performance using the NGO model. NGO mimics the behavioural mechanisms of Northern Goshawks naturally when pursuing prey, incorporating exploitation and exploration stages to optimise and achieve fast convergence; the iterative stages are as demonstrated [21].

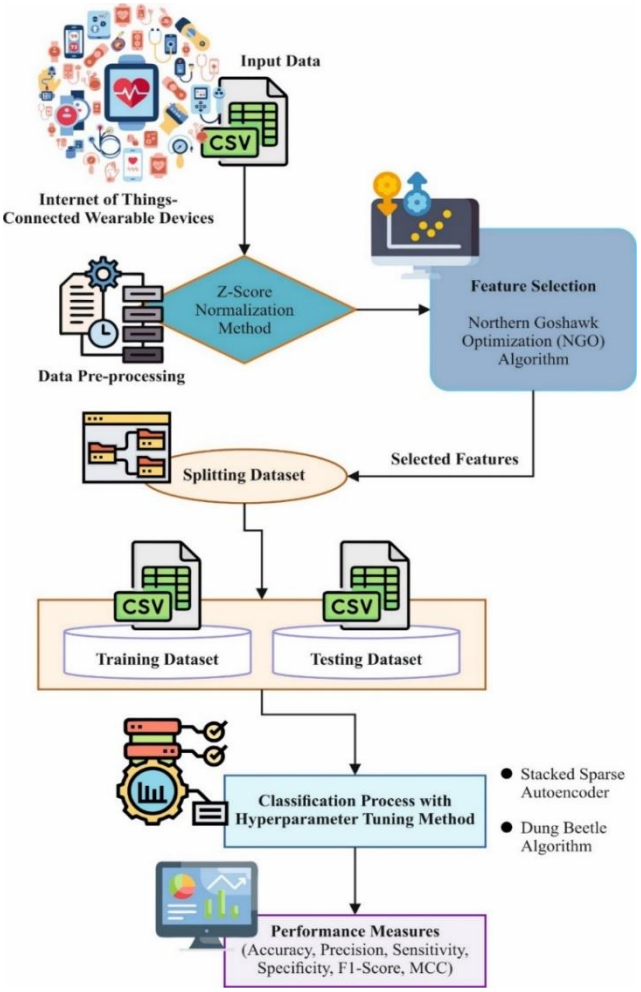

Fig.2. Complete workflow of MWD-DSAEOA model

3.2.1 Population Initialisation Stage:

Every goshawk is considered a vector, and therefore a collection of goshawks generates the population matrix of the model. The members of the population are randomly initialised inside the searching area.

$$C = \begin{bmatrix} C_1 \\ \vdots \\ C_i \\ \vdots \\ C_N \end{bmatrix} = \begin{bmatrix} C_{1,1} & \cdots & C_{1,j} & \cdots & C_{1,M} \\ \vdots & \vdots & \vdots & \vdots & \vdots \\ C_{i,1} & \cdots & C_{i,j} & \cdots & C_{i,M} \\ \vdots & \vdots & \vdots & \ddots & \vdots \\ C_{N,1} & \cdots & C_{N,j} & \cdots & C_{N,M} \end{bmatrix} \tag{2}$$

where, C characterises the Northern Goshawk's population, C_i means primary location of the i^{th} goshawk; $C_{i,j}$ refers to the area of the i^{th} goshawk in the j^{th} size; N and M correspond to the size of the population and the dimension of the objective function, respectively.

The column vector makes up the objective function. While $F(C)$ denotes a vector of the objective function, F_i denotes the objective function corresponding to the i^{th} targeted location.

$$F(C)=\begin{bmatrix} F_1=F(C_1) \\ \vdots \\ F_i=F(C_i) \\ \vdots \\ F_N=F(C_N) \end{bmatrix}_{N\times 1} \tag{3}$$

3.2.2 *Randomly identification of primary locations of the Northern Goshawks:*

$$C_{i,j}=lb_j+r(ub_j-lb_j) \tag{3}$$

whereas lb_j and ub_j signify upper and lower limits, and $r\in[0,1]$ means a randomly generated number.

3.2.3 *Estimate the population:*

Assessing every goshawk, recording the best place of every searching goshawk, and upgrading their locations according to the objective function.

3.2.4 *Identification and Exploration Stage:*

NG randomly select prey for fast attacks and fine-tunes their positions based on fitness values.

$$P_i=C_k,\quad i=1,2,\ldots,N;k=1,2,\ldots,i-1,\ldots,N$$

$$C_{i,j}^{new,P_1}=\begin{cases} C_{i,j}+q(p_{i,j}-SC_{i,j}), & F_{P_i}<F_i \\ C_{i,j}+q(C_{i,j}-p_{i,j}), & F_{P_i}<F_i \end{cases}$$

$$C_i=\begin{cases} C_i^{new,P_1}, & F_i^{new,P_1}<F_i \\ C_i, & F_i^{new,P_1}\geq F_i \end{cases} \tag{5}$$

whereas P_i refers to the prey location attacked by the i^{th} goshawk; F_{P_i} signify the function of the objective; C_i^{new,P_1} denote the upgraded location of the i^{th} goshawk at the present step; C_i^{new,P_1} means the novel area of the goshawk in the j^{th} size; F_i^{new,P_1} indicate the objective function at this novel place. $q\in[0,1]$ and S=1,2 can improve the searching ability.

3.2.5 *Development and Hunting Stage:*

The NG rapidly hunts the prey inside the circular searching radius of R. Let C_i^{new,P_2} refer to the new position of the i^{th} goshawk within the j^{th} size; T specifies the maximal number of iterations; C_i^{new,P_2} denote the novel location of the goshawk in the predatory stage; and F_i^{new,P_2} means the function value at the novel area of the prey.

$$C_{i,j}^{new,P_2}=C_{i,j}+R(2r-1)C_{i,j}$$

$$R=0.02\left(1-\frac{t}{T}\right)$$

$$C_i=\begin{cases} C_i^{new,P_2}, & F_i^{new,P_2}<F_i \\ C_i, & F_i^{new,P_2}\geq F_i \end{cases} \tag{6}$$

Upgrade the locations and fitness of individuals within the population and check the maximum number of iterations or the end condition. Save the optimal solution and its location, then output the result.

The fitness function (FF) applied aims to balance the designated feature values in each solution (minimum) with the classifier's precision (maximum) achieved using these selected attributes. Eq. (7) exemplifies the FF for assessing solutions.

$$Fitness=\alpha\gamma_R(D)+\beta\frac{|R|}{|C|} \tag{7}$$

whereas $\gamma_R(D)$ indicates the classifier's error rate. $|R|$ denotes the cardinality of the selected subset, $|C|$ denotes the complete feature count, and α and β are two parameters.

3.3 SSAE-BASED HEALTHCARE DATA MONITORING

In addition, the classification process primarily uses the SSAE method. AEs are artificial neural networks (ANNs) mainly used for unsupervised learning and can extract latent features from raw data [22].

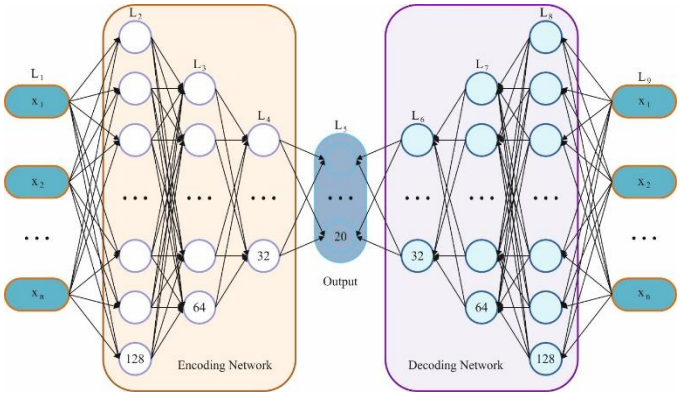

Fig.3. Architecture of the SSAE model

During this AE framework, input data is converted into a simplified representation. The target is to maintain sufficient critical information to overcome this bottleneck and facilitate noise reduction and data compression. An essential mechanism involves an NN reconstructing the primary input data to reduce the discrepancy between matrices H and X. This discrepancy was measured as the reconstruction error, as expressed in the equation below. The standard AE framework includes three layers. The latent layer helps summarise the recently generated feature data, represented by H. The structure splits into two parts: the encoder that converts X to H. The decoding reconstructs H reverse into $\hat{X}$ as mentioned below in the equations.

$$L(X,\hat{X})=\frac{1}{n}\sum_{i=1}^{n}\| x_i-\hat{x}_i \|^2 \tag{8}$$

$$H=f(WX+b) \tag{9}$$

$$\hat{X}=g(W'H+b') \tag{10}$$

where, b and W represent the bias vector and weight matrix, respectively. W' and b' signify the consistent parameters. $F(\cdot)$ and $G(\cdot)$ symbolise the active function.

Therefore, the major AEs are combined to form a stacked AE (SAE). It involves directly connecting the output of a single layer to the input of the following layer sequentially. Moreover, to alleviate the risks of overfitting and unnecessary feature learning, an SSAE is presented by incorporating sparse constraints within the modelling structure. These sparse limits are applied to the outputs of latent-layer neurons to examine the intrinsic

architecture of the data, efficiently suppressing the state of activation after the output estimates zero. The SSAE uses L1 regularisation to enforce sparsity within the primary objective function defined in Eq. (11).

$$J_{SSA}(W,b) = \frac{1}{n}\sum_{i=1}^{n} \| x_i - \hat{x}_i \|^2 + \lambda \| W \|_1 \quad (11)$$

where, λ indicates the regularisation coefficient. W epitomises 1-regularization. The Fig.3 signifies the structure of the SSAE model.

3.4 FINE-TUNING USING OPTIMISATION APPROACH

To improve the model performance, the DBO is used for parameter tuning. The DBO model targets the discovery of optimal solutions through ball rolling, dancing, breeding, foraging, and stealing movements [23]. Consequently, this model has four processes: rolling balls, foraging, stealing, and breeding.

3.5 DB BALL ROLLING

In this setting, the DB relies on the sun's location to preserve the rolling path directly. The location of DB was upgraded utilising the below equation:

$$x_i(t+1) = x_i(t) + \alpha \cdot k \cdot x_i(t-1) + b \cdot \Delta x$$
$$\Delta x = | x_i(t) - X^w | \quad (12)$$

where, the current iteration and the recent DB location are represented as t and $x_i(t)$, respectively. a describes the abnormality of the DB from the normal route. It captures two values at random: 1 or -1, while 1 and -1 denote that deviation is absent and present, respectively. k-value is between 0 and 0.2. b is restricted to (0,1). The poor global value is denoted as X^w, and the representation of solar lighting is denoted Δx; thus, a large Δx value might imply a great distance from the sources of light. The tangent function is used to find the original ball-rolling path when a problem arises, mimicking the DB's dancing behaviour. Then, the location of the rolling DB was designated below:

$$x_i(t+1) = x_i(t) + \tan(\theta) | x_i(t) - x_i(t-1) | \quad (13)$$

The parameter θ lies in the interval $[0, \pi]$. If θ equals 0, $\pi/2$, or π, no location modification occurs; thus, it is not upgraded.

3.6 SPAWNING DBS

In their real-world setting, DBs are mainly prone to spawn in safe areas. This tactic considers choosing secure borders in the location to characterise safe places and is specified as shown:

$$Lb^* = \max(X^*(1-R), Lb)$$
$$Ub^* = \min(X^*(1-R), Ub) \quad 914)$$

The spawning area boundaries are specified by Lb^* and Ub^*. X^* signifies the present local optimum, whereas the parameter of convergence R is described as $1-t/T$, where T denotes the maximal iteration limit. Then, once the DB identifies the top breeding site, it will select a location within the specified range to lay its eggs.

$$X_i(t+1) = X^* + b_1(X_i(t) - Lb^*) + b_2(X_i(t) - Ub^*) \quad (15)$$

While b_1 and b_2 are random vectors, all having a dimension of 1xd, whereas d specifies the optimiser size.

3.7 FORAGING DBS

In this setting, once they select a secure area, foraging is more closely linked to egg-laying and therefore occurs only near that region.

$$Lb^b = \max(X^b(1-R), Lb)$$
$$Ub^b = \min(X^b(1+R), Ub) \quad (16)$$

whereas, X^b will reflect an optimum global location. Ub^b and Lb^b characterise the restrictions on the foraging area correspondingly. In addition, Lb and Ub characterise the field range for problem-solving.

$$x_i(t+1) = x_i(t) + C_1(x_i(t) - Lb^b) + C_2(x_i(t) - Ub^b) \quad (17)$$

where the variable C_1 emulates standard distributions, C_2 refers to a vector of dimensions 1xd, where d indicates the dimensionality of the problem, with elements ranging between (0,1).

3.8 STEALING DBS

In their natural environment, DBs in particular areas are not accurately pinched from other DBs; instead, they contend for possession by transferring them. Therefore, in the primary hunt, they utilised the top global location, X^b, as an estimate of such behaviour. The thieving DB moves to relocate itself, like the position update as stated by Eq. (18):

$$x_i(t+1) = X^b + S \cdot g \cdot (| x_i(t) - X^* | + | x_i(t) - X^b |) \quad (18)$$

where, assume S refers to a constant of 0.5, and g denotes the dimension of the arbitrary variable. The DBO initiates an FF to improve classification performance. It presents an optimistic estimate of the improved outcome of candidate solutions. Here, the reduction in the classifier's error rate is measured as the FF.

$$fitness(x_i) = ClassifierErrorRate(x_i)$$
$$= \frac{\text{number of misclassified instances}}{\text{total number of instances}} \times 100 \quad (19)$$

3.9 EVALUATION METRICS

To estimate the performance of this predictive method for drug-target interaction, a range of metrics was applied to assess the presented method for the interaction prediction tasks. These metrics provide a comprehensive understanding of the model's reliability and effectiveness.

- Accuracy: The percentage of accurately classified samples (either positive or negative) devoid of complete prediction.

$$Accuracy = \frac{T_r P + T_r N}{T_r P + F_l P + T_r N + F_l N} \quad (20)$$

- Precision: It estimates the precision of positive prediction, established by separating the actual positive counts by the amount of either positives or true or false.

$$Precision = \frac{T_r P}{T_r P + F_l P} \quad (21)$$

- Sensitivity: The capability of the method to properly recognise positive samples.

$$Sensitivity = \frac{T_r P}{T_r P + F_l N} \quad (22)$$

- Specificity: The capability of the method to properly recognise negative samples.

$$Specificity = \frac{T_r N}{T_r N + F_l P} \tag{23}$$

- F1 Score: The harmonic mean of Precision and Recall, balancing the trade-off between false negatives and false positives.

$$F1\text{-}Score = \frac{2(Precision \cdot Recall)}{Precision + Recall} \tag{24}$$

- Matthews Correlation Coefficient (*MCC*): It is a coefficient of correlation between predicted and real binary classification. On a scale of -1 to 1, 1 signifies the best prediction, −1 signifies complete disagreement, and 0 signifies an arbitrary prediction. It is measured by balancing amounts, even after addressing an unbalanced database.

$$MCC = \frac{(T_r P \times T_r N) - (F_l P \times F_l N)}{\sqrt{(T_r P + F_l P)(T_r P + F_l N)(T_r N + F_l P)(T_r N + F_l N)}} \tag{25}$$

4. RESULT ANALYSIS AND DISCUSSIONS

The performance of the PMWD-DSAEOA model is evaluated using Healthcare IoT data [24]. This database suggests sensor data collected from wearable devices in an IoT-based healthcare system. The data matches patient health monitoring with sensors that determine numerous essential signs. These sensors, such as temperature, blood pressure, heart rate, and battery level, provide real-time information that is transmitted to healthcare providers for remote monitoring. This dataset includes 200 instances across two health statuses, as shown in Table 2 below. There are 13 features, but only nine are selected.

Table.2. Details of the dataset

Status of Health	No. of Instances
"Unhealthy (in essential medical attention)"	113
"Healthy"	87
Total Instances	**200**

The Fig.4 portrays the classifier performance of the PMWD-DSAEOA model. The Fig.4a reveals the 80% TRPHE of the confusion matrix with precise classification and recognition of each class label. The Fig.4b shows the PR analysis, indicating the optimal outcome for each class label. Finally, Fig.4c demonstrates the ROC analysis, suggesting capable solutions with superior ROC values across diverse classes.

The Fig.5 depicts the classifier solution of the PMWD-DSAEOA method. The Fig.5a shows the 20% TSPHE of the confusion matrix, with precise classification and recognition of each class. The Fig.5b presents the PR analysis, specifying the optimal threshold for each class label. Eventually, Fig.5c establishes the ROC analysis, suggesting strong performance with higher ROC values across various classes.

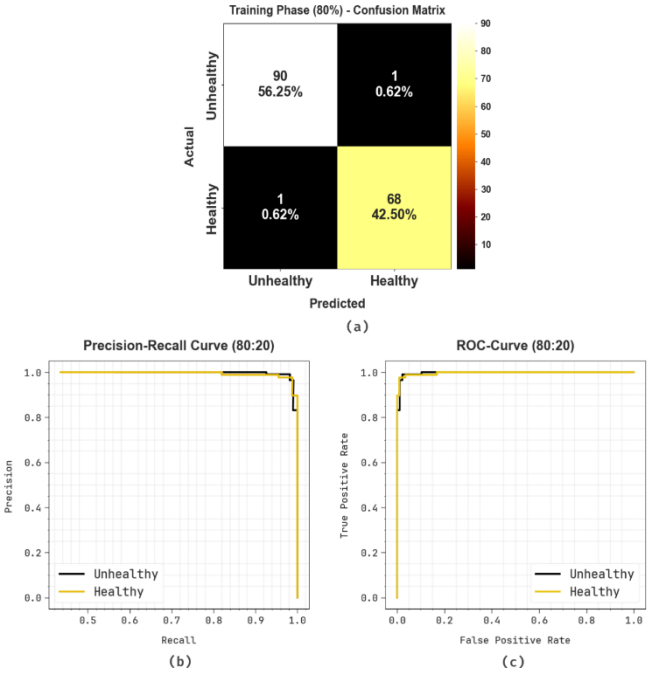

Fig.4. Classifier outcome of PMWD-DSAEOA model (a) 80% confusion matrix and (b, c) PR and ROC curves of 80:20

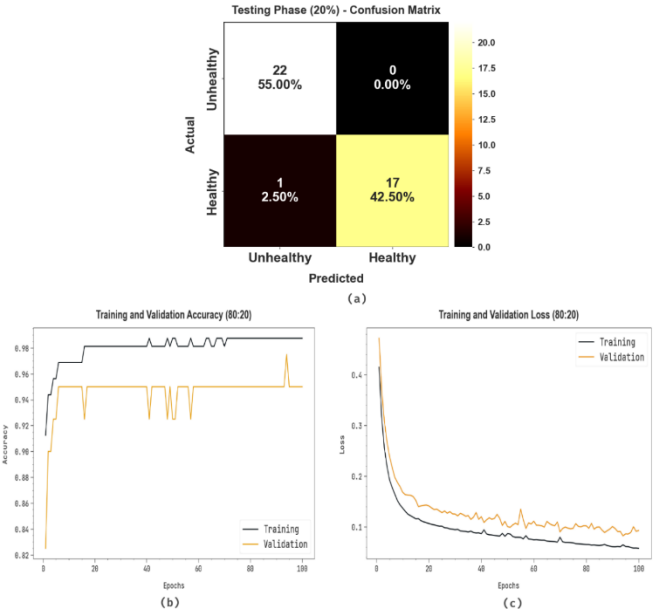

Fig.5. Classifier outcome of PMWD-DSAEOA model (a) 20% confusion matrix and (b, c) PR and ROC curves of 80:20

The Table.3 and Fig.6 denote the health monitoring performance of the PMWD-DSAEOA method under 80:20. Under 80%TRPHE, the PMWD-DSAEOA approach gains an average $accur_y$, $preci_n$, $sens_y$, $spec_y$, $F1_{Score}$, and *MCC* of 98.73%, 98.73%, 98.73%, 98.73%, 98.73%, and 97.45%, correspondingly. Moreover, on 20%TSPHE, the PMWD-DSAEOA approach achieves average $accur_y$, $preci_n$, $sens_y$, $spec_y$, $F1_{Score}$, and *MCC* of 97.22%, 97.83%, 97.22%, 97.22%, 97.46%, and 95.05%, respectively.

Table.3. Health monitoring of PMWD-DSAEOA model under 80:20

Class Labels	$accur_y$	$preci_n$	$sens_y$	$spec_y$	$F1_{Score}$	MCC
TRPHE (80%)						
Unhealthy	98.90	98.90	98.90	98.55	98.90	97.45
Healthy	98.55	98.55	98.55	98.90	98.55	97.45
Average	**98.73**	**98.73**	**98.73**	**98.73**	**98.73**	**97.45**
TSPHE (20%)						
Unhealthy	100.00	95.65	100.00	94.44	97.78	95.05
Healthy	94.44	100.00	94.44	100.00	97.14	95.05
Average	**97.22**	**97.83**	**97.22**	**97.22**	**97.46**	**95.05**

Fig.6. Average values of PMWD-DSAEOA model under 80:20

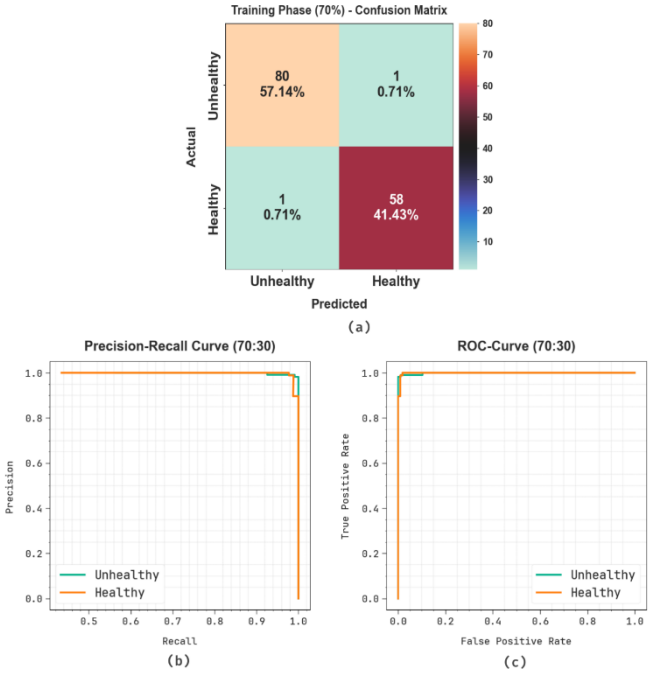

Fig.7. Classifier outcome of PMWD-DSAEOA model (a) 70% confusion matrix and (b, c) PR and ROC curves of 70:30

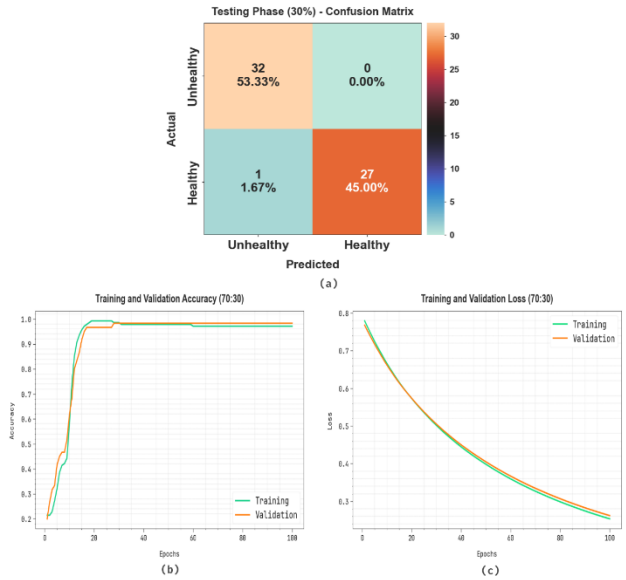

Fig.8. Classifier outcome of PMWD-DSAEOA methodology (a) 30% confusion matrix and (b, c) PR and ROC curves of 70:30

The Fig.7 illustrates the classifier result of the PMWD-DSAEOA model. The Fig.7a shows the 70% TRPHE of the confusion matrix, with precise classification and identification of each class. The Fig.7b shows the PR analysis, indicating the optimal outcome for each class label. Finally, Fig.7c presents the ROC analysis, indicating a capable solution with the highest ROC value across numerous classes.

The Fig.8 portrays the classifier performance of the PMWD-DSAEOA methodology. The Fig.8a shows the 30% TSPHE of the confusion matrix, with precise classification and identification of each class. The Fig.8b shows the PR analysis, suggesting better outcomes for each class label. Eventually, Fig.8c depicts the ROC analysis, showing strong performance with higher ROC values across numerous class labels.

The Table 4 and Fig.9 depict the health monitoring result of the PMWD-DSAEOA approach under 70:30. Under 70%TRPHE, the PMWD-DSAEOA approach attains an average $accur_y$, $preci_n$, $sens_y$, $spec_y$, $F1_{Score}$, and MCC of 98.54%, 98.54%, 98.54%, 98.54%, 98.54%, and 97.07%, correspondingly. Furthermore, on 30%TSPHE, the PMWD-DSAEOA methodology attains average $accur_y$, $preci_n$, $sens_y$, $spec_y$, $F1_{Score}$, and MCC of 98.21%, 98.48%, 98.21%, 98.21%, 98.32%, and 96.70%, respectively.

Table.4. Health monitoring of PMWD-DSAEOA approach under 70:30

Class Labels	$accur_y$	$preci_n$	$sens_y$	$spec_y$	$F1_{Score}$	MCC
TRPHE (70%)						
Unhealthy	98.77	98.77	98.77	98.31	98.77	97.07
Healthy	98.31	98.31	98.31	98.77	98.31	97.07
Average	**98.54**	**98.54**	**98.54**	**98.54**	**98.54**	**97.07**
TSPHE (30%)						
Unhealthy	100.00	96.97	100.00	96.43	98.46	96.70
Healthy	96.43	100.00	96.43	100.00	98.18	96.70
Average	**98.21**	**98.48**	**98.21**	**98.21**	**98.32**	**96.70**

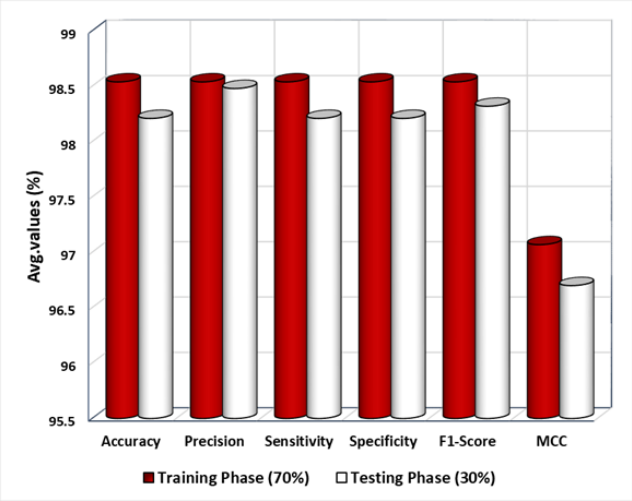

Fig.9. Average values of the PMWD-DSAEOA approach under 70:30

Table.5. Comparative study of PMWD-DSAEOA approach with existing models

Approaches	$accur_y$	$preci_n$	$sens_y$	$spec_y$	$F1_{Score}$
ETs	91.67	93.97	87.90	89.23	94.88
KNN Algorithm	85.23	92.87	86.90	95.43	97.17
LR	93.60	97.29	97.95	97.68	90.70
XGboost	97.34	96.15	90.36	93.59	96.19
EDN-SVM	97.93	86.88	94.97	92.87	85.48
AI-IoT Method	96.45	98.47	86.33	93.06	91.63
HMS-ITM	93.09	97.52	95.56	93.64	87.35
PMWD-DSAEOA	98.73	98.73	98.73	98.73	98.73

The Table.5 presents a comparative study of the PMWD-DSAEOA model with recent methods across various metrics [25-27].

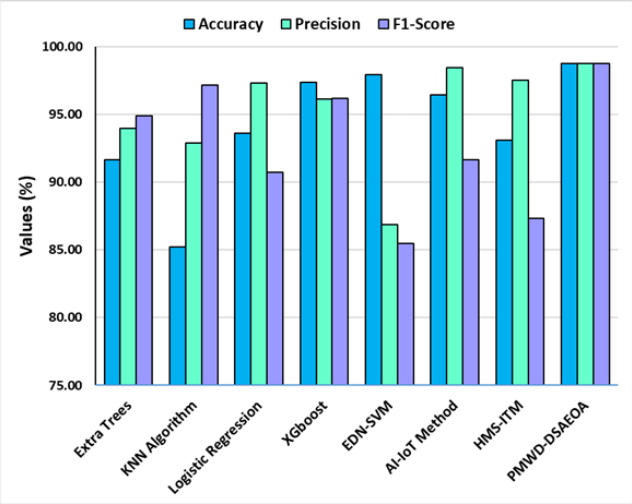

Fig.10. $accur_y$, $preci_n$ and $F1_{Score}$, outcome of the PMWD-DSAEOA approach with existing models

The Fig.10 presents the simulation performance of the PMWD-DSAEOA method compared with existing techniques in terms of $accur_y$, $preci_n$ and $F1_{Score}$. Based on $accur_y$, the PMWD-DSAEOA method has achieved an $accur_y$ of 98.73%. In contrast, the Extra Trees (ET), K-Neural Network (KNN), Logistic Regression (LR), XGboost, EDN-SVM, AI-IoT, and HMS-ITM models have reached a minimal $accur_y$ of 91.67%, 85.23%, 93.60%, 97.34%, 97.93%, 96.45%, and 93.09%, correspondingly. In addition, based on $F1_{Score}$, the PMWD-DSAEOA method has achieved a superior $F1_{Score}$ of 98.73% although the ETs, KNN, LR, XGboost, EDN-SVM, AI-IoT, and HMS-ITM models have accomplished minimal $F1_{score}$ of 94.88%, 97.17%, 90.70%, 96.19%, 85.48%, 91.63%, and 87.35%, correspondingly.

The Fig.11 presents the $sens_y$ and $spec_y$ outcomes of the PMWD-DSAEOA method compared with existing techniques. Based on $sens_y$, the PMWD-DSAEOA method has a maximal $sens_y$ of 98.73% although the ETs, KNN, LR, XGboost, EDN-SVM, AI-IoT, and HMS-ITM approaches have achieved a lower $sens_y$ of 87.90%, 86.90%, 97.95%, 90.36%, 94.97%, 86.33%, and 95.56%, correspondingly. In addition, based on $spec_y$, the PMWD-DSAEOA methodology has obtained a greater $spec_y$ of 98.73%. In contrast, the ETs, KNN, LR, XGboost, EDN-SVM, AI-IoT, and HMS-ITM approaches have achieved a lower $spec_y$ of 89.23%, 95.43%, 97.68%, 93.59%, 92.87%, 93.06%, and 93.64%, respectively.

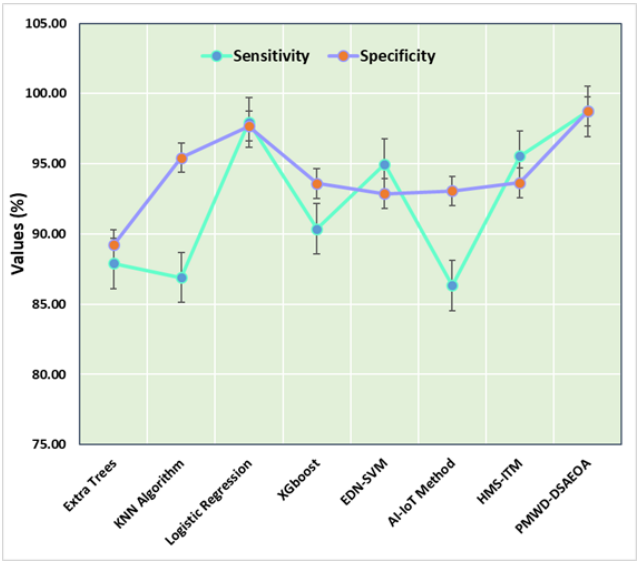

Fig.11. $sens_y$ and $spec_y$ outcome of the PMWD-DSAEOA method with existing models

Table.6. CT outcome of PMWD-DSAEOA methodology with existing approaches

Approaches	CT (sec)
ETs	91.67
KNN Algorithm	85.23
LR	93.60
XGboost	97.34
EDN-SVM	97.93
AI-IoT Method	96.45
HMS-ITM	93.09
PMWD-DSAEOA	98.73

Fig.12. CT (s) outcome of PMWD-DSAEOA methodology with existing approaches

In Table 6 and Fig.12, the comparison results for the PMWD-DSAEOA approach are reported in terms of computational time (CT). The solution recommends that the PMWD-DSAEOA approach yield better outcomes. Based on CT, the PMWD-DSAEOA methodology yields a lower CT of 98.73sec, while the ETs, KNN, LR, XGboost, EDN-SVM, AI-IoT, and HMS-ITM models achieve superior CT values of 91.67sec, 85.23sec, 93.60sec, 7.34sec, 97.93sec, 96.45sec, and 93.09sec, respectively.

5. CONCLUSIONS

In this paper, a PMWD-DSAEOA approach is proposed in smart healthcare. The paper aims to design an effective system for real-time health monitoring using wearable devices to enable proactive, tailored healthcare solutions. For that purpose, the PMWD-DSAEOA approach comprises a data pre-processing step by using Z-score normalisation to standardise the input data for effective analysis. Then, the feature selection step is applied, which is crucial because it reduces data dimensionality and improves the model's efficacy. In addition, the classification process primarily uses the SSAE method. To further enhance the model's performance, the DBO is applied for parameter tuning. To demonstrate the PMWD-DSAEOA model's enhanced performance, a broad experimental study is conducted. The comparative outcomes indicated the model's improved features.

REFERENCES

[1] N. Surantha, P. Atmaja and M. Wicaksono, "A Review of Wearable Internet-of-Things Device for Healthcare", *Procedia Computer Science*, Vol. 179, pp. 936-943, 2021.

[2] M.A. Akkas, R. Sokullu and H.E. Çetin, "Healthcare and Patient Monitoring using IoT", *Internet of Things*, Vol. 11, pp. 1-6, 2020.

[3] S.D. Mamdiwar, R. Akshith, Z. Shakruwala, U. Chadha, K. Srinivasan and C.Y. Chang, "Recent Advances on IoT-Assisted Wearable Sensor Systems for Healthcare Monitoring", *Biosensors*, Vol. 11, No. 10, pp. 1-6, 2021.

[4] L.A. Duran-Vega, P.C. Santana-Mancilla, R. Buenrostro-Mariscal, J. Contreras-Castillo, L.E. Anido-Rifón, M.A. García-Ruiz, O.A. Montesinos-Lopez and F. Estrada-Gonzalez, "An IoT System for Remote Health Monitoring in Elderly Adults through a Wearable Device and Mobile Application", *Geriatrics*, Vol. 4, No. 2, pp. 1-9, 2019.

[5] H.S. Saad, J.F. Zaki and M.M. Abdelsalam, "Employing of Machine Learning and Wearable Devices in Healthcare System: Tasks and Challenges", *Neural Computing and Applications*, Vol. 36, No. 29, pp. 17829-17849, 2024.

[6] A.R. Nasser, A.M. Hasan, A.J. Humaidi, A. Alkhayyat, L. Alzubaidi, M.A. Fadhel, J. Santamaría and Y. Duan, "Iot and Cloud Computing in Health-Care: A New Wearable Device and Cloud-based Deep Learning Algorithm for Monitoring of Diabetes", *Electronics*, Vol. 10, No. 21, pp. 1-5, 2021.

[7] B. Pradhan, S. Bhattacharyya and K. Pal, "IoT-based Applications in Healthcare Devices", *Journal of Healthcare Engineering*, Vol. 2021, No. 1, pp. 1-8, 2021.

[8] L. Lu, J. Zhang, Y. Xie, F. Gao, S. Xu, X. Wu and Z. Ye, "Wearable Health Devices in Health Care: Narrative Systematic Review", *JMIR mHealth and uHealth*, Vol. 8, No. 11, pp. 1-7, 2021.

[9] E.A. Adeniyi, R.O. Ogundokun and J.B. Awotunde, "IoMT-based Wearable Body Sensors Network Healthcare Monitoring System", *IoT in Healthcare and Ambient Assisted Living*, pp. 103-121, 2021.

[10] P. Bhambri and A. Khang, "Managing and Monitoring Patient's Healthcare using AI and IoT Technologies", *Driving Smart Medical Diagnosis through AI-Powered Technologies and Applications*, pp. 1-23, 2024.

[11] A. Souri, M.Y. Ghafour, A.M. Ahmed, F. Safara, A. Yamini and M. Hoseyninezhad, "A New Machine Learning-based Healthcare Monitoring Model for Student's Condition Diagnosis in Internet of Things Environment", *Soft Computing*, Vol. 24, No. 22, pp. 17111-17121, 2020.

[12] M. Anjum, N. Kraiem, H. Min, A.K. Dutta, Y.I. Daradkeh and S. Shahab, "Opportunistic Access Control Scheme for Enhancing IoT-Enabled Healthcare Security using Blockchain and Machine Learning", *Scientific Reports*, Vol. 15, No. 1, pp. 1-6, 2025.

[13] W. Rafique, "ML-RASPF: A Machine Learning-based Rate-Adaptive Framework for Dynamic Resource Allocation in Smart Healthcare IoT", *Algorithms*, Vol. 18, No. 6, pp. 1-7, 2025.

[14] A. Aldosary and M. Tanveer, "PAAF-SHS: PUF and Authenticated Encryption based Authentication Framework for the IoT-Enabled Smart Healthcare System", *Internet of Things*, Vol. 26, pp. 1-9, 2024.

[15] A. Rahman, M.A.H. Wadud, M.J. Islam, D. Kundu, T.A.U.H. Bhuiyan, G. Muhammad and Z. Ali, "Internet of Medical Things and Blockchain-Enabled Patient-Centric Agent through SDN for Remote Patient Monitoring in 5G Network", *Scientific Reports*, Vol. 14, No. 1, pp. 1-5, 2024.

[16] A. Balasundaram, S. Routray, A.V. Prabu, P. Krishnan, P.P. Malla and M. Maiti, "Internet of Things (IoT)-based Smart Healthcare System for Efficient Diagnostics of Health Parameters of Patients in Emergency Care", *IEEE Internet of Things Journal*, Vol. 10, No. 21, pp.18563-18570, 2023.

[17] R.R. Irshad, S.S. Sohail, S. Hussain, D.O. Madsen, A.S. Zamani, A.A.A. Ahmed, A.A. Alattab, M.M. Badr and I.M. Alwayle, "Towards Enhancing Security of IoT-Enabled Healthcare System", *Heliyon*, Vol. 9, No. 11, pp. 1-5, 2023.

[18] N. Gharaei, Y.D. Al-Otaibi, S.J. Malebary and A.O. Almagrabi, "A Storage Optimisation and Energy-Efficiency-based Edge-Enabled Companion-Side eHealth Monitoring System for IoT-based Smart Hospitals", *IEEE*

Internet of Things Journal, Vol. 11, No. 2, pp. 3628-3638, 2023.

[19] K. Paulraj, N. Soms, S.D.S. Azariya and V. Sureshkumar, "Smart Healthcare Monitoring System: Integrating IoT, Deep Learning, and XGBoost for Real-Time Patient Diagnosis", *Proceedings of International Conference on Information Technology*, pp. 708-713, 2023.

[20] E.M. Priya and K.S. Krishnan, "Life-Care: IoT-Cloud-Enabled Smart Heart Disease Prediction System for Smart Healthcare Environment using Deep Learning", *International Journal of Distributed Sensor Networks*, Vol. 2025, No. 1, pp. 1-7, 2025.

[21] H. Ma, M.S.M. Kasihmuddin, M.A. Mansor, S.Z.M. Jamaludin, M.F. Marsani and F.Z.C. Rose, "Hybrid OCSSA-VMD and Optimized Deep Learning Networks for Runoff Forecasting", *IEEE Access*, pp. 1-6, 2025.

[22] C. Yao, X. Kong, L. Tang and X. Ling, "An Unsupervised Deep Learning Surrounding Rock Perception Method for TBM Operational Parameter Multiobjective Optimisation", *Results in Engineering*, Vol. 35, pp. 1-5, 2025.

[23] M. Abdel-Salam, D. Oliva, M. Perez-Cisneros and I.M. El-Hasnony, "Advanced Feature Selection Approach with Halton-based Enhanced Adaptive Dung Beetle Algorithm", *Cluster Computing*, Vol. 28, No. 9, pp. 1-7, 2025.

[24] "Healthcare IOT Data", Available at https://www.kaggle.com/datasets/ziya07/healthcare-iot-data, Accessed in 2025.

[25] G. Singh, "Wearable IoT (W-IoT) Artificial Intelligence (AI) Solution for Sustainable Smart-Healthcare", *International Journal of Information Management Data Insights*, Vol. 5, No. 1, pp. 1-7, 2025.

[26] M. Zonayed, "Machine Learning and IoT in Healthcare: Recent Advancements, Challenges and Future Direction", *Proceedings of International Conference on Advances in Biomarker Sciences and Technology*, pp. 1-7, 2025.

[27] R.R. Irshad, S. Hussain, I. Hussain, A.A. Alattab, A. Yousif, O.A.S. Alsaiari and E.I.I. Ibrahim, "A Novel Artificial Spider Monkey based Random Forest Hybrid Framework for Monitoring and Predictive Diagnoses of Patients Healthcare", *IEEE Access*, Vol. 11, pp. 77880-77894, 2023.